KUNS-1373
HE(TH) 95/23
hep-ph/9512375

CHIRAL SYMMETRY RESTORATION AT FINITE TEMPERATURE AND CHEMICAL POTENTIAL IN THE IMPROVED LADDER APPROXIMATION

Yusuke Taniguchi * and Yuhsuke Yoshida †

Department of Physics, Kyoto University
Kyoto 606-01, Japan

Abstract

The chiral symmetry of QCD is studied at finite temperature and chemical potential using the Schwinger-Dyson equation in the improved ladder approximation. We calculate three order parameters; the vacuum expectation value of the quark bilinear operator, the pion decay constant and the quark mass gap. We have a second order phase transition at the temperature $T_c = 169$ MeV along the zero chemical potential line, and a first order phase transition at the chemical potential $\mu_c = 598$ MeV along the zero temperature line. We also calculate the critical exponents of the three order parameters.

PACS numbers 11.10.Wx, 11.15.Tk, 11.30.Qc, 11.30.Rd, 12.38.-t .

*e-mail address : tanigchi@gauge.scphys.kyoto-u.ac.jp
†e-mail address : yoshida@gauge.scphys.kyoto-u.ac.jp

1 Introduction

The chiral symmetry in QCD is dynamically broken at zero temperature. This feature is confirmed by the fact that the pion is the Nambu-Goldstone boson accompanied with this symmetry breaking. On the other hand, it is shown that spontaneously broken symmetries restore at sufficiently high temperature (and/or chemical potential) in some simple models.[1] Then, the same restoration is also expected to hold for the dynamically broken chiral symmetry in QCD. This phenomena is widely believed to be seen in heavy-ion collisions, the early universe and the neutron stars.

There are various attempts to study the phase diagram and critical behavior. In order to do them we need any non-perturbative treatments such as ε or $1/N$ expansion, lattice simulation, the Schwinger-Dyson equation and so on. Based on universality arguments it is expected that critical phenomena of finite temperature QCD is described by a three dimensional linear σ model with the same global symmetry, in which the ε expansion is used.[2] Lattice simulations are powerful tools to study the QCD at finite temperature.[3, 4, 5, 6] The Schwinger-Dyson equation in the improved ladder approximation is solved with further approximations and give the dynamical symmetry restoration.[7, 8, 9, 10, 11] Nambu-Jona-Lasinio models, as phenomenological models of QCD, provide us with useful pictures about the dynamical chiral symmetry breaking and its restoration.[12, 13, 14] In these three approaches it is indicated that there is a second order phase transition at $(T, \mu) = (T_c, 0)$ and a first order one at $(T, \mu) = (0, \mu_c)$ in the case of the two massless flavors. The phase transition points are found to be of order $T_c \sim 200$, $\mu_c \sim 400$ MeV.

In this paper we use the Schwinger-Dyson equation in the improved ladder approximation. The advantages of this approach are that it is a convenient tool to study the nature of the chiral symmetry, and we easily introduce fermions coupling to the gluon in the chiral limit at finite temperature and chemical potential. Further, we have no degrees of freedom (parameters) to fit the physical observables, and we obtain a definite answer.

In previous attempts further approximations are introduced in addition to the ladder approximation. Some non-perturbative approximation can violate the chiral symmetry, and reliable results cannot be obtained. We would like to obtain the results keeping the chiral symmetry within the framework of the Schwinger-Dyson equation only in the improved ladder approximation.

We calculate the values of the three order parameters; the quark mass gap, the vacuum expectation value of the quark bilinear operator $\langle\overline{\psi}\psi\rangle$ and the pion decay constant. We have a second order phase transition at $T_c = 169$ MeV along the $\mu = 0$ line and a first order phase transition at $\mu_c = 598$ MeV along the $T = 0$ line. The critical exponents of

the above three order parameters are extracted at $(T, \mu) = (T_c, 0)$, which shows that our formulation is different from mean field theories.

This paper is organized as follows. In section 2, we show basic ingredients to study the chiral symmetry restoration using the Schwinger-Dyson equation in the improved ladder approximation. The expressions of the three order parameters are given in terms of the quark mass function. The Pagels-Stokar formula is used to calculate the pion decay constant. In section 3 we give our numerical results. The Schwinger-Dyson equation is numerically solved using a iteration method. We determine the positions and the orders of phase transitions. We also extract the critical exponents. Summary and discussion are found in section 4.

2 Schwinger-Dyson Equation at Finite Temperature and Chemical Potential

The restoration of spontaneously broken symmetry occurs at finite temperature and chemical potential.[1] The phenomena is described in terms of the imaginary time formalism in gauge theories.[15, 16]

In this section we show basic ingredients to solve the Schwinger-Dyson equation at finite temperature and chemical potential. Then, we study the dynamical chiral symmetry breaking and its restoration. In this paper all dimensionful quantities are rescaled by using the Λ_{QCD}, otherwise stated.

We consider the QCD with massless u and d quarks, and then there is a $SU(2)_L \times SU(2)_R$ chiral symmetry. There are several probes to investigate the chiral symmetry such as the quark mass gap, the vacuum expectation value of the quark bilinear operator (VEV) and the decay constant of the pion. Those are evaluated in terms of the quark mass function $\Sigma(p)$. The mass function is determined by the Schwinger-Dyson equation. We use the improved ladder approximation to solve this equation. We work with three flavor β-function for the running coupling, since the s quark also contributes to the running of the coupling in the concerned energy range.

At zero temperature this approximation provides us with a convincing result of the dynamical chiral symmetry breaking and good values of the lowest-lying meson masses. So, we expect that the approximation gives good result even in the case of finite temperature.

To take the effect of finite temperature into account, we work in the imaginary time formalism[15, 16]. Let us start with writing down the Schwinger-Dyson equation as in Fig. 1. The diagram is exactly the same as that in the zero temperature QCD, since the difference between the usual (zero temperature) field theory and finite temperature field

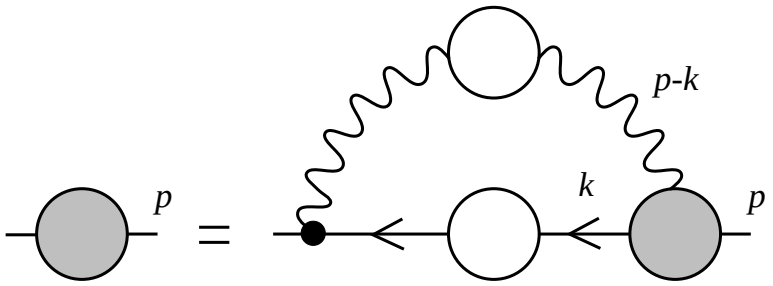

Figure 1: The Feynman diagram of the Schwinger-Dyson equation. We have the same diagram for the equation at finite temperature and chemical potential.

theory stems from the boundary effect of time only. The time components of quark and gluon momenta become discrete. Since quark fields have anti-periodic boundary condition in the imaginary time direction, we have

$$\begin{aligned} p^0 &= 2\pi i T\left(n+\frac{1}{2}\right) \ , \\ k^0 &= 2\pi i T\left(m+\frac{1}{2}\right) \ , \end{aligned} \tag{2.1}$$

where $n, m \in \boldsymbol{Z}$. When the chemical potential μ is introduced, the time component of p in the quark propagator $S_F(p)$ is modified as

$$p_0 \to p_0 - \mu \ . \tag{2.2}$$

The momentum integration is modified to the summation:

$$\int \frac{d^4k}{(2\pi)^4 i} \quad \to \quad T\sum_{m=-\infty}^{\infty} \int \frac{d^3k}{(2\pi)^3} \ . \tag{2.3}$$

Then, modifying the Schwinger-Dyson equation at zero temperature according to Eqs. (2.1), (2.2) and (2.3), the Schwinger-Dyson equation at finite temperature is given as

$$\not{p} - S_F(p)^{-1} = T\sum_{m=-\infty}^{\infty} \int \frac{d^3k}{(2\pi)^3} C_2 g^2(p,k) K_{\mu\nu}(p-k)\gamma^\mu S_F(k)\gamma^\nu \ , \tag{2.4}$$

where C_2 is the second Casimir invariant and $-K_{\mu\nu}$ is the gluon tree propagator in the Landau gauge:

$$K_{\mu\nu}(l) = \frac{1}{-l^2}\left(g_{\mu\nu} - \frac{l_\mu l_\nu}{l^2}\right) \ . \tag{2.5}$$

The quantity $g^2(p,k)$ is a one-loop running coupling depending on the momenta p and k. In order to describe a property of QCD we use the following form for the running

coupling:[17]

$$g^2(p,k) = \frac{1}{\beta_0} \times \begin{cases} \dfrac{1}{t} & \text{if } t_F < t \\ \dfrac{1}{t_F} + \dfrac{(t_F - t_C)^2 - (t - t_C)^2}{2t_F^2(t_F - t_C)} & \text{if } t_C < t < t_F \\ \dfrac{1}{t_F} + \dfrac{(t_F - t_C)}{2t_F^2} & \text{if } t < t_C \end{cases} , \tag{2.6}$$

where $t = \ln(p^2+k^2)$, $t_C \equiv -2.0$, $\beta_0 = (11N_c - 2N_f)/(48\pi^2)$ is the coefficient of one-loop β-function and t_F is a parameter needed to regularize the divergence of the running coupling at the QCD scale Λ_{QCD}. We call t_F the infrared regularization parameter. $N_c = 3$ and $N_f = 3$ are the number of colors and flavors, respectively. The running coupling g^2 is smoothly interpolated between the ordinary one-loop running coupling form at $t > t_F$ and a constant value in the low energy region. As will be shown, the results do not depend on this particular infrared regularization. By virtue of the running effect of the coupling the resultant mass function, which is determined by Eq. (2.4), reproduces the exact behavior in the high energy region.[18] Notice that this property is needed to preserve the chiral symmetry.[19]

The quark propagator is expanded by three $SO(3)$ invariant amplitudes as

$$S_F(p) = \frac{1}{\Sigma(p) + (\mu + B(p))\gamma^0 - A(p)\not{p}} . \tag{2.7}$$

At the vanishing temperature and chemical potential limits ($T, \mu \to 0$) the choice of Landau gauge allows us to obtain

$$\begin{aligned} A(p) &= 1 , \\ B(p) &= 0 . \end{aligned} \tag{2.8}$$

Although we are studying in finite temperature and chemical potential, we assume the relations (2.8) for simplicity. We expect that the relation (2.8) is not changed so much in the case of low temperature and chemical potential. As shown later, the phase transition line of the chiral symmetry restoration lies in that region; $T_c, \mu_c \lesssim \Lambda_{QCD}$. Then, the result should not change qualitatively.

Now, substituting Eq. (2.7) into Eq. (2.4) under the condition (2.8), we obtain

$$\Sigma_n(x) = \sum_{m=-\infty}^{\infty} \int y dy K_{nm}(x,y) \frac{\Sigma_m(y)}{\left(2\pi T(m+\frac{1}{2}) + i\mu\right)^2 + y^2 + \Sigma_m(y)^2} , \tag{2.9}$$

where $x = |\boldsymbol{p}|$ and $y = |\boldsymbol{k}|$ and

$$K_{nm}(x,y) = \frac{3TC_2 g^2(p,k)}{8\pi^2 xy} \ln\left(\frac{4\pi^2T^2(n-m)^2 + (x+y)^2}{4\pi^2T^2(n-m)^2 + (x-y)^2}\right) . \tag{2.10}$$

Notice that we have the $SO(3)$ rotational invariance but not $SO(3,1)$. The mass function $\Sigma(p)$ is a function of p^0 and $\boldsymbol{p}^2$, and is rewritten as $\Sigma_n(x)$. In the presence of the chemical potential we easily find from Eq. (2.9) that the mass function takes a complex value satisfying the relation

$$\Sigma_{-n}(x)^* = \Sigma_{n-1}(x) \quad \text{for} \quad n = 1, 2, \cdots \ . \tag{2.11}$$

We solve the Schwinger-Dyson equation (2.9) numerically by an iteration (relaxation) method. The momentum valuables x, y are discretized to be

$$x \quad \to \quad x_n = \exp\left(\Lambda_{IR} + (\Lambda_{UV} - \Lambda_{IR})\frac{n-1}{N_{SD}-1}\right) \ , \tag{2.12}$$

where $n = 1, 2, \cdots, N_{SD}$ and similarly for y. We divide $\ln x$ and $\ln y$ into N_{SD} points. The quantity $\Lambda \equiv \exp \Lambda_{UV}$ defines the ultraviolet cutoff for the space component of momenta. Therefore an $SO(3)$ symmetric cutoff Λ is introduced, which is needed for numerical calculation. The momentum region of the time component is properly truncated so that the support of the mass function is covered well, as well as that of the space component. We have integrable singularities at $(n, x) = (m, y)$ stemming from the tree level gluon pole, but these should be regularized in the numerical calculation. In order to avoid this singularity we apply a two-point splitting prescription

$$K_{nm}(x, y) \quad \to \quad \frac{1}{2}\Big(K_{nm}(x, y_+) + K_{nm}(x, y_-)\Big) \ , \tag{2.13}$$

with $y_\pm = y \exp(\pm(\Lambda_{UV} - \Lambda_{IR})/(4N_{SD}))$. The validity of this prescription is checked by using the conventional (zero temperature) Schwinger-Dyson equation.

After obtaining the mass function, we immediately evaluate the pion decay constant by using the Pagels-Stokar formula at finite temperature:

$$f_\pi(T,\mu)^2 = \frac{2N_c T}{\pi^2}\sum_n \int_0^\infty x^2 dx \, \frac{\Sigma_n(x)\Big(\Sigma_n(x) - \dfrac{x}{3}\dfrac{d\Sigma_n(x)}{dx}\Big)}{\Big(\Big(2\pi T(n+\frac{1}{2}) + i\mu\Big)^2 + x^2 + \Sigma_n(x)^2\Big)^2} \ . \tag{2.14}$$

We also calculate the VEV

$$\langle \overline{u}u \rangle_\Lambda = \langle \overline{d}d \rangle_\Lambda = \frac{2N_c T}{\pi^2}\sum_n \int_0^\Lambda x^2 dx \, \frac{\Sigma_n(x)}{\Big(2\pi T(n+\frac{1}{2}) + i\mu\Big)^2 + x^2 + \Sigma_n(x)^2} \ . \tag{2.15}$$

The VEV is renormalized at 1 GeV via

$$\langle \overline{\psi}\psi \rangle_{1\mathrm{GeV}} = \left(\frac{\ln(1\mathrm{GeV})}{\ln \Lambda}\right)^{\frac{11N_c - 2N_f}{9C_2}} \langle \overline{\psi}\psi \rangle_\Lambda \ , \tag{2.16}$$

where $\psi = u, d$.

3 Numerical Results

In this section we solve the Schwinger-Dyson equation numerically by an iteration method. We start with an initial form of the mass function and input it in the R.H.S. of Eq.(2.9). Performing the integration of x and the summation of n, we have an updated form of the mass function, which is taken as a more suitable trial form. After sufficient iterations the functional form converges giving the true solution with enough accuracy. The convergence of the solution is very rapid off the phase transition regions. A typical form of the mass function is shown in Fig. 2 at $T = 90$, $\mu = 0$ MeV. The mass function dumps so fast in

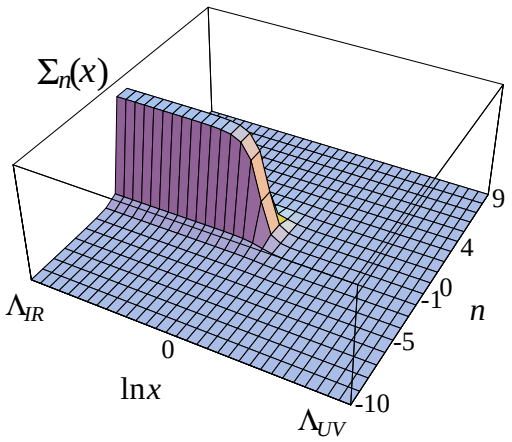

Figure 2: A typical form of the mass function. We put $T = 90$, $\mu = 0$ MeV. The integer n specifies the time component of the momentum as in Eq. (2.1) and x is given in Eq. (2.12).

the $p_4 \equiv -ip_0$ direction that the values of the mass function at $n \gtrsim 4$ are much smaller than that at $n = 0$ ($\Sigma_n(x) \sim 10^{-2} \times \Sigma_0(x)$). This implies a dimensional reduction at sufficiently high temperature; i.e., four dimensional theory at finite temperature belongs to the same universality class as that of a three dimensional one with the same symmetry.

We use the VEV and the pion decay constant as order parameters of the chiral symmetry. The dynamical mass of the quark itself is also an order parameter.

We determine the value of Λ_{QCD} from the experimental result $f_\pi = 93$ MeV at $T = \mu = 0$, and we have $\Lambda_{QCD} = 592$ MeV using Eq. (2.14) at $t_F = 0.5$. This is our result of Λ_{QCD} obtained by using the one-loop β-function. In this paper we put the infrared regularization parameter $t_F = 0.5$ and show later that the physical observables as well as the phase transition line do not depend on t_F.

3.1 Zero chemical potential case

First, we study the phase transition along the $\mu = 0$ line. The phase transition point is defined so that three order parameters of the mass gap $\Sigma_{n=0}(x = 0)$, the VEV $\langle\overline{\psi}\psi\rangle$ and the pion decay constant f_π vanish. We show the temperature dependences of these order parameters in Fig. 3 with two massless flavors. The $SU(2)_L \times SU(2)_R$ chiral symmetry

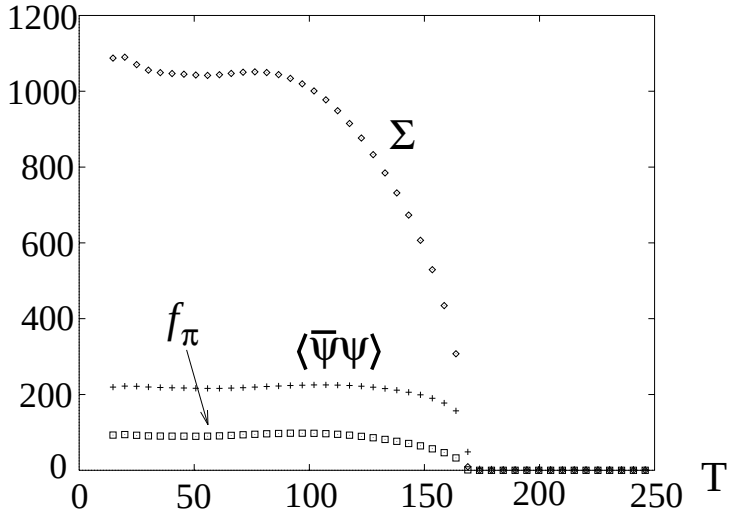

Figure 3: The functional forms of the order parameters (the mass function, the VEV and the pion decay constant) for T along the $\mu = 0$ line.

restores at $T = T_c = 169$ MeV. We have a second order phase transition. We have the same result as that of lattice simulations[5, 6] with two flavors in which the phase transition is second order at $T_c \sim 200$ MeV.

The ladder approximation, used here, gives no flavor dependence, since the dependence essentially comes through only the running effect of the coupling. Whereas the flavor dependence is suggested by the universality arguments[2] and it is confirmed by lattice simulations[3, 5, 6], where we have a second order phase transition at $N_f = 2$ and first order ones at $N_f \geq 3$. The Nambu-Jona-Lasinio models[12, 13, 14] imply that the inclusion of the effect of $U(1)_A$ anomaly, so called the instanton effect, allows us to obtain the same flavor dependence as that in the lattice simulations.

The important point in studying the chiral symmetry is that the approximation used should preserve the symmetry. Fortunately, the ladder approximation itself is consistent with the chiral symmetry.[19] However, many investigations violate the chiral symmetry, where further approximations are used in addition to the ladder[7, 9, 10]. In order to reserve the symmetry the high energy behavior of the quark mass function must be

consistent with the result of the operator product expansion (OPE):[19]

$$\Sigma_n(\boldsymbol{p}^2) \sim \frac{g^2(x)}{x} (\ln x)^{\frac{9C_2}{11N_c-2N_f}} \quad \text{as} \quad x \equiv p_4^2 + \boldsymbol{p}^2 \sim \infty \ . \tag{3.1}$$

Here we should notice that even in the finite temperature case the high energy behavior of the mass function is the same as that of zero temperature case, since the temperature effect is suppressed in the high energy region. In Refs. [7, 9, 10] their further approximation (Σ = const.) does not satisfy Eq. (3.1), on the other hand in Ref. [11] they adopt an ansatz consistent with Eq. (3.1) up to the logarithmic correction. While our formalism exactly reproduce the OPE result (3.1).

We check the dependence of the order parameters on the infrared regularization parameter t_F. The physical observables, $\langle\overline{\psi}\psi\rangle_{1\mathrm{GeV}}$ and $f_\pi(T)$, should not depend on the parameter t_F. We confirm this requirement. The dependence of the VEV and the $f_\pi(T)$ are shown in Figs. 4 and 5. The values of the VEV and the f_π change, at worst, by 5%

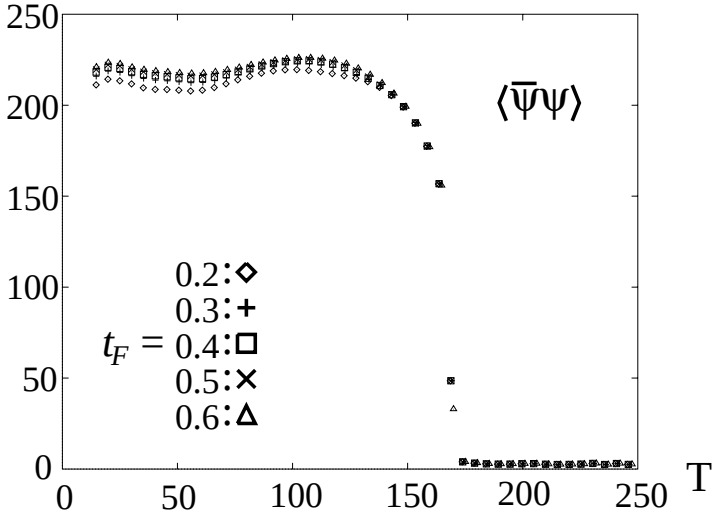

Figure 4: The t_F dependence of the VEV. It changes by 5% at worst against t_F.

and 8% against $t_F = 0.2 \sim 0.6$, respectively. These values of $t_F = 0.2 \sim 0.6$ correspond to those of the running coupling $g^2(p{=}k{=}0) = 570 \sim 92.6$. Moreover, the phase transition point is fairly stable against t_F. We conclude that there is no t_F dependence of the physical observables and the position of the phase transition point.

We also show the dependence of the mass function in Fig. 6. We have a strong t_F dependence. Since the mass function is not a physical observable it may depend on the regularization parameter t_F. However the phase transition point determined using the mass function is fixed.

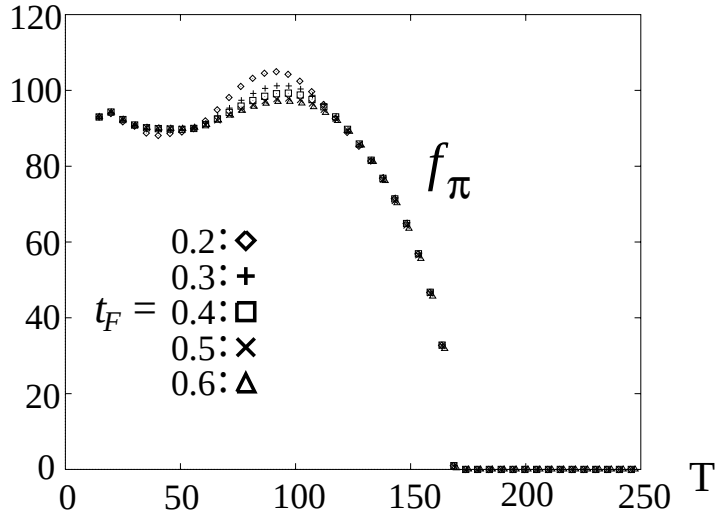

Figure 5: The t_F dependence of the pion decay constant. It changes by 8% at worst against t_F.

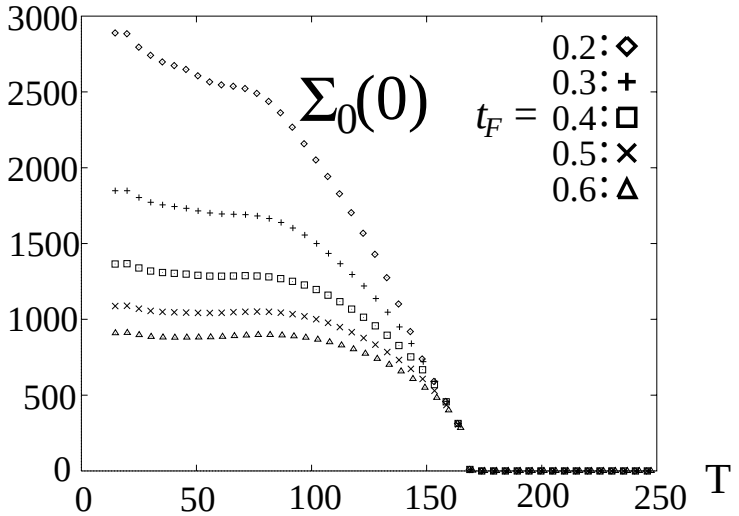

Figure 6: The t_F dependence of the mass function. We have a strong dependence.

Let us examine the critical behavior of the system. Since we have a second order phase transition at $(T, \mu) = (T_c, 0)$, the three order parameters behave near the phase transition point as

$$\begin{aligned} \langle\overline{\psi}\psi\rangle_{1\mathrm{GeV}} &\sim \left(1 - \frac{T}{T_c}\right)^{\beta} , \\ \Sigma_0(0) &\sim \left(1 - \frac{T}{T_c}\right)^{\nu} , \\ f_\pi(T) &\sim \left(1 - \frac{T}{T_c}\right)^{\beta'} , \end{aligned} \tag{3.2}$$

where $T < T_c$. The critical exponents β, ν and β' are numerically extracted by using the χ^2 fitting. The order parameters $\mathcal{O}$ $(= \langle\overline{\psi}\psi\rangle_{1\mathrm{GeV}}, \Sigma_0(0), f_\pi(T))$ are fitted by the linear functional form $\ln \mathcal{O}(T) = A + \gamma \ln(1 - T/T_c)$, and the fitting parameters are A and γ $(= \beta, \nu, \beta')$ with $T_c = 169$ MeV. We have good fittings, which is shown in Fig. 7. The result is

$$\beta = 0.171 \ , \quad \nu = 0.497 \ , \quad \beta' = 0.507 \ . \tag{3.3}$$

These values are different from those in mean field theories. If we consider mean field theories, we would have the relation $\beta = \nu$ since $\Sigma \sim \langle\overline{\psi}\psi\rangle$.

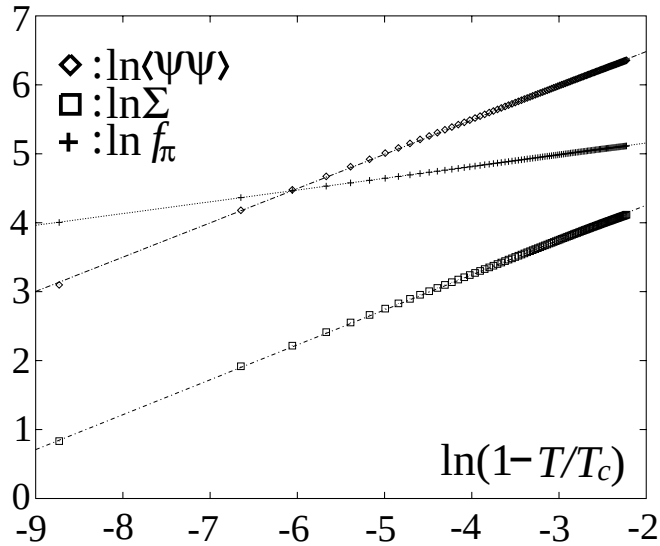

Figure 7: The χ^2 fittings for extracting the critical exponents of the VEV, the mass gap and the pion decay constant. We draw the best fitted lines of the form $A + \gamma \ln(1 - T/T_c)$.

3.2 Zero temperature case

Next, we study the phase transition along the $T = 0$ line. As is seen from Eq. (2.9), the mass function has an imaginary part for $\mu \neq 0$. The functional forms for μ are shown of the VEV, the pion decay constant $f_\pi(\mu)$, the real and the imaginary parts of the mass gap in Figs. 8 and 9. The $SU(2)_L \times SU(2)_R$ chiral symmetry restores at $\mu = \mu_c = 598$

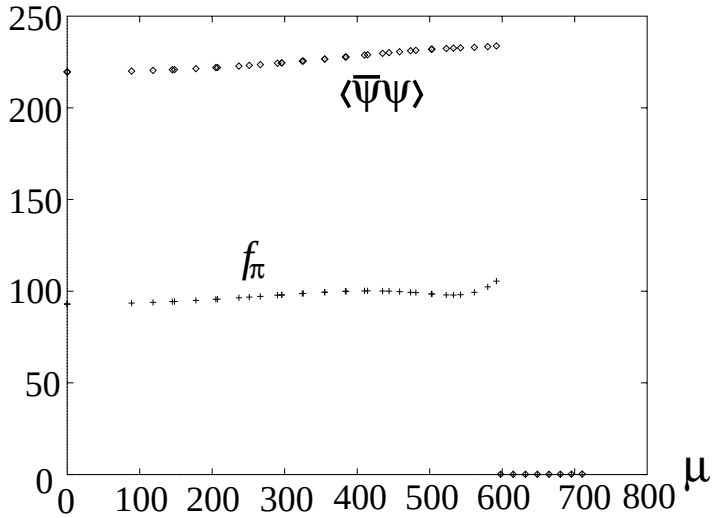

Figure 8: The functional forms of the VEV and the pion decay constant for μ along $T = 0$ line.

MeV. We have a strong first order phase transition. Here, we check that the infrared regularization parameter t_F does not affects the physical observables and the nature of the phase transition.

Let us compare our result with those of other approaches. There is no lattice simulation at so large chemical potential that we can directly see the phase transition. A phase transition is suggested by extrapolating the result of lattice simulation around small μ.[4] On the other hand, there are many attempts using Schwinger-Dyson equations[7, 9, 11] and NJL models[13, 14]. The previous attempts[9, 11] in the ladder approximation give a first order phase transition. The NJL[13, 14] models with the instanton effect also give the same at $N_f = 2, 3$. Therefore, our result confirms theirs. Our advantage is that we have no parameter which modifies the physical result.

3.3 the phase diagram

Finally, we study the phase diagram of the chiral symmetry restoration. Near the $\mu = 0$ line we have second order phase transitions and near the $T = 0$ line we have first order ones. In both cases the convergences of updating the mass function are rapid well for

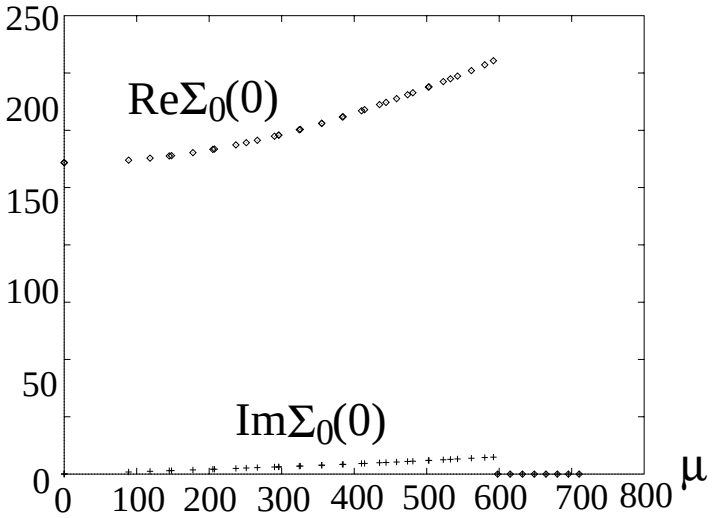

Figure 9: The functional forms of the real and the imaginary parts of the mass function for μ along $T = 0$ line.

solving the Schwinger-Dyson equation. Unfortunately, near the phase transition line in the middle region, the convergences are too bad to obtain solutions with a suitable accuracy. However, an natural guess will be that the order of phase transitions continuously changes from first order to second order, through weak first order, in the middle region shown as in Fig. 10. This type of diagram is also obtained in Refs. [11, 13], which is the same as that of two dimensional Gross-Neveu model in Refs. [20, 21].

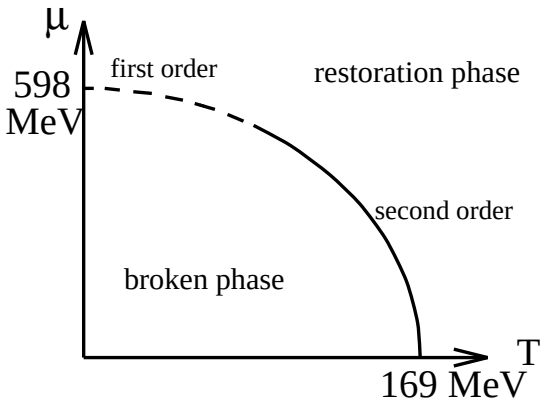

Figure 10: The schematic view of the phase diagram from our result.

4 Summary and Discussion

In this paper we study the chiral symmetry restoration at finite temperature and chemical potential in QCD. We use the improved ladder approximation and the imaginary time

formalism. The improved ladder approximation does not violate the chiral symmetry, since the high energy behavior of the quark mass function is consistent with the result of the operator product expansion[19] even at finite temperature and chemical potential. The phase transition point (or line) is determined by using the three order parameters; i.e., the VEV $\langle\overline{\psi}\psi\rangle_{1\mathrm{GeV}}$ renormalized at 1 GeV, the quark mass gap $\Sigma_0(0)$ and the pion decay constant f_π. In the improved ladder approximation the infrared regularization parameter t_F must be introduced as in Eq. (2.6) in order to regularize the running coupling. We, however, observe that the physical quantities do not depend on the parameter t_F. Then, our results are obtained without any degrees of freedom other than Λ_{QCD} which is determined by putting $f_\pi = 93$ MeV at $(T, \mu) = (0, 0)$.

In the case of the vanishing chemical potential $\mu = 0$ we have a second order phase transition at $T_c = 169$ MeV. The critical exponents are extracted in Eq. (3.3). This shows that the QCD in the improved ladder approximation is different from mean field theories. In the case of the vanishing temperature $T = 0$ we have a strong first order phase transition at $\mu = 598$ MeV.

In the $(T, \mu) = (0, 0)$ limit the functional forms $A(p) = 1$ and $B(p) = 0$ as in Eq. (2.8) give the solution of the Schwinger-Dyson equation in Landau gauge. In this paper we put these forms for any (T, μ) for simplicity. We should check the validity of this prescription. In the middle region ($0 < T < T_c$ and $0 < \mu < \mu_c$) near the phase transition line the calculation of the mass function is too hard for the error to vanish in the iteration method. It is necessary to obtain more efficient method for solving the Schwinger-Dyson equation in this region. After these problems being settled, the framework of the improved ladder approximation becomes a more convenient tool to figure out the nature of chiral symmetry, since it is easy to introduce fermions in the chiral limit.

Acknowledgements

We would like to thank T. Hatsuda and Y. Kikukawa for valuable discussions and comments.

References

[1] D.A. Kirzhnits and A.D. Linde, *Phys. Lett.* **42B** (1972) 471;
S. Weinberg, *Phys. Rev.* **D9** (1974) 3357;
L. Dolan and R. Jackiw, *Phys. Rev.* **D9** (1974) 3320.

[2] R.D. Pisarski and F. Wilczek, *Phys. Rev.* **D29** (1984) 338;
K. Rajagopal and F. Wilczek, *Nucl. Phys.* **B399** (1993) 395.

[3] J. Polonyi, H.W. Wyld, J.B. Kogut, J. Shigemitsu and D.K. Sinclair *Phys. Rev. Lett.* **53** (1984) 644;
R. Gupta, G. Guralnik, G.W. Kilcup, A. Patel and S.R. Sharpe, *Phys. Rev. Lett.* **57** (1986) 2621;
E.V. Kovacs, D.K. Sinclair and J.B. Kogut, *Phys. Rev. Lett.* **58** (1987) 751.

[4] J. Kogut, H. Matsuoka, M. Stone, H.W. Wyld, S. Shenker, J. Shigemitsu and D.K. Sinclair, *Nucl. Phys.* **B225** (1983) 93;
J.B. Kogut, M.P. Lombardo and D.K. Sinclair, *Phys. Rev.* **D51** (1995) 1282.

[5] F.R. Brown, F.P. Butler, H. Chen, N.H. Christ, Z. Dong, W. Schaffer, L.I. Unger and A. Vaccarino, *Phys. Rev. Lett.* **65** (1990) 2491.

[6] Y. Iwasaki, K. Kanaya, S. Sakai and T. Yoshie, *Nucl. Phys.* **B34** (Proc. Suppl.) (1994).

[7] D. Bailin, J. Cleymans and M.D. Scadron, *Phys. Rev.* **D31** (1985) 164.

[8] A. Kocić, *Phys. Rev.* **D33** (1986) 1785.

[9] T. Akiba, *Phys. Rev.* **D36** (1987) 1905.

[10] T.S. Evans and R.J. Rivers, *Z. Phys.* **C40** (1988) 293.

[11] A. Barducci, R. Casalbuoni, S.De Curtis, R. Gatto and G. Pettini,
Phys. Rev. **D41** (1990) 1610; *Phys. Lett.* **B240** (1990) 429.

[12] T. Hatsuda and Kunihiro, *Phys. Rev. Lett.* **55** (1985) 158; *Prog. Theor. Phys.* **74** (1985) 765; *Phys. Lett* **B198** (1987) 126.

[13] M. Asakawa and K. Yazaki, *Nucl. Phys.* **A504** (1989) 668.

[14] M. Lutz, S. Klimt and W. Wise, *Nucl. Phys.* **A542** (1992) 521.

[15] T. Matsubara, *Prog. Theoret. Phys.* **14** (1955) 351;
C.W. Bernard, *Phys. Rev.* **D9** (1974) 3312;
H. Hata and T. Kugo, *Phys. Rev.* **D21** (1980) 3333.

[16] R.P. Feynman and A.R. Hibbs, *"Quantum Mechanics and Path Integrals"*, McGraw-Hill, New York, 1965;
A.L. Fetter and J.D. Walecka, *"Quantum Theory of Many-Particle Systems"*, McGraw-Hill, New York, 1971.

[17] K.-I. Aoki, M. Bando, T. Kugo, M.G. Mitchard and H. Nakatani, *Prog. Theor. Phys.* **84** (1990) 683.

[18] H.D. Politzer, *Nucl. Phys.* **B117** (1976) 397.

[19] K. Higashijima, *Phys. Rev.* **D29** (1984) 1228;
V.A. Miransky, *Sov. J. Nucl. Phys.* **38** (1984) 280.

[20] U. Wolff, *Phys. Lett.* **157B** (1985) 303.

[21] T. Inagaki, T. Kouno and T. Muta, *Int. J. Mod. Phys.* **A10** (1995) 2241.